

Optimization of Nonatitanate Electrodes for Sodium-Ion Batteries

Judith Alvarado^{1,\$}, Gözde Barim^{1,\$}, Calvin D. Quilty², Eongyu Yi¹, Kenneth J. Takeuchi^{2,3}, Esther S. Takeuchi^{2,3,4}, Amy C. Marschilok^{2,3,4}, Marca M. Doeff^{1,*}

1. Energy Storage & Distributed Resources Division, Lawrence Berkeley National Laboratory, Berkeley, CA 94720.
2. Department of Chemistry, Stony Brook University, Stony Brook, NY 11794.
3. Department of Materials Science and Chemical Engineering, Stony Brook University, Stony Brook, NY 11794.
4. Energy and Photon Sciences Directorate, Brookhaven National Laboratory, Upton, NY 11973.

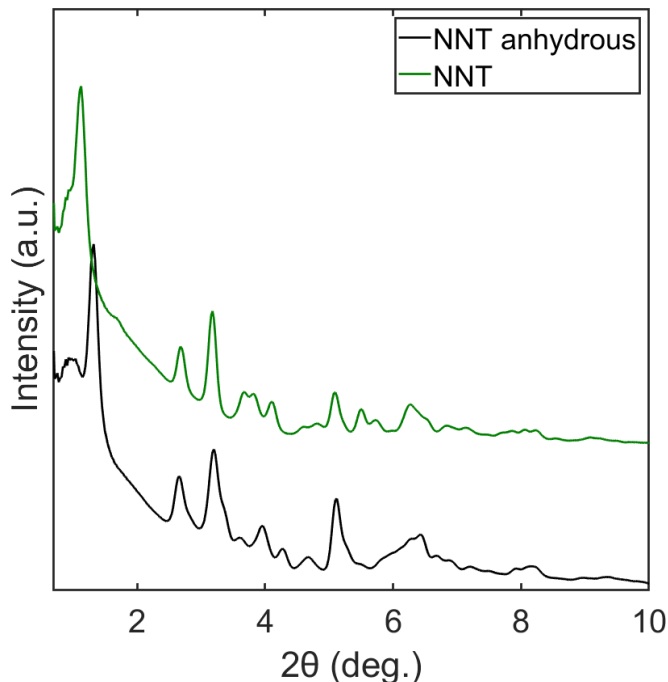


Fig. S1. XRD patterns of as prepared NNT and anhydrous NNT (annealed at 600 °C).

Table S1. Rietveld refinements of XRD patterns of as prepared NNT, anhydrous NNT, as prepared NNT-GO, and anhydrous NNT-GO.

Material	As prepared NNT	Anhydrous NNT	As prepared NNT-GO	Anhydrous NNT-GO
Formula	NaTi ₃ O ₆ OH·2H ₂ O	NaTi ₃ O ₆ OH	NaTi ₃ O ₆ OH·2H ₂ O	NaTi ₃ O ₆ OH
Space group	C/2m	C/2m	C/2m	C/2m
<i>a</i> (Å)	21.4(3)	20.8(4)	21.5(1)	21.5(7)
<i>b</i> (Å)	3.741(2)	3.793(5)	3.747(1)	3.767(4)
<i>c</i> (Å)	12.0(1)	10.6(1)	11.99(4)	11.1(2)
β (°)	135.8(2)	137.1(3)	135.96(9)	138.3 (5)
Cryst. Size (nm, eq.)	>200 nm	>200 nm	>200 nm	>200 nm
Cryst. Size (nm, ax.)	22(3)	15(2)	32(4)	8.0(7)
%R _{wp}	2.49	4.63	2.82	3.55

Table S2. Atomic positions of as prepared NNT determined by Rietveld refinement.

Atom	<i>x</i>	<i>y</i>	<i>z</i>	Wyckoff Site
Na	0.759(5)	0	0.896(8)	4i
Ti1	0.75463(2)	0	0.391(2)	4i
Ti2	0.584(3)	0.5	0.517(4)	4i
Ti3	0.564(2)	0	0.291(4)	4i
O1	0.741(6)	0	0.60(1)	4i
O2	0.629(8)	0	0.21(2)	4i
O3	0.660(7)	0.5	0.61(1)	4i
O4	0.599(8)	0.5	0.38(1)	4i
O5	0.565(4)	0.5	0.658(9)	4i
O6	0.528(6)	0	0.42(1)	4i
O-H	0.452(7)	0	0.11(1)	4i
O-H ₂	0.329(5)	0	0.080(9)	4i
O-H ₂	0.877(7)	0	0.88(1)	4i

Table S3. Atomic positions of anhydrous NNT determined by Rietveld refinement.

Atom	<i>x</i>	<i>y</i>	<i>z</i>	Wyckoff Site
Na	0.83(2)	0.25(5)	0.02(4)	8j
Ti1	0.7420(2)	0	0.393(6)	4i
Ti2	0.573(5)	0.5	0.56(1)	4i
Ti3	0.563(4)	0	0.293(7)	4i
O1	0.73(1)	0	0.55(3)	4i
O2	0.62(1)	0	0.22(3)	4i
O3	0.752(8)	0.5	0.69(2)	4i
O4	0.61(2)	0.5	0.22(3)	4i
O5	0.58(2)	0.5	0.72(3)	4i
O6	0.58(2)	0	0.52(5)	4i
O-H	0.34(4)	0.25(9)	0.07(5)	8j

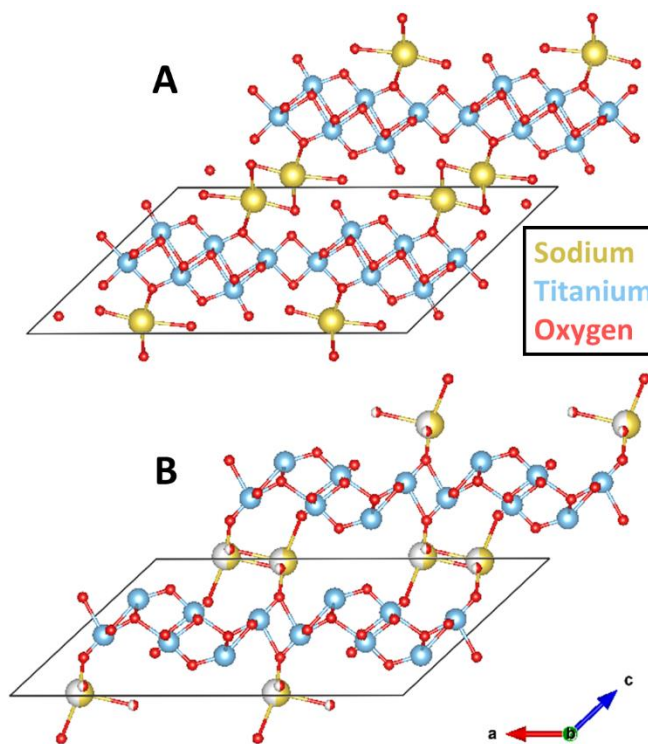


Fig. S2. Crystal structures of (a) NNT as prepared and (b) NNT annealed at 600 °C.

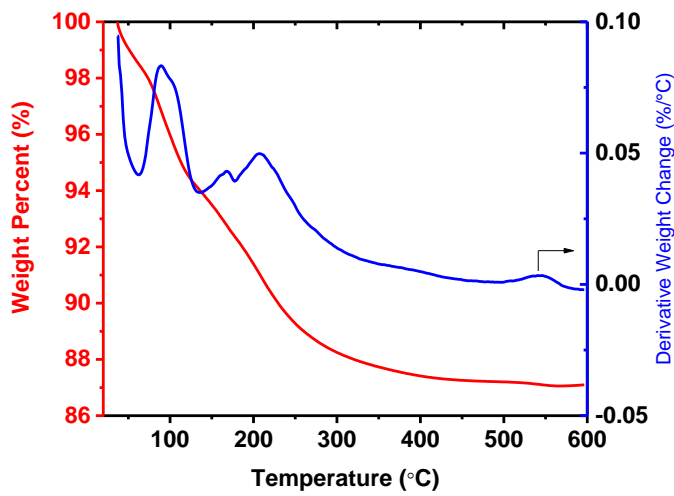


Fig. S3. Thermogravimetric analysis of as-prepared NNT under nitrogen using a heating rate of 5 °C/minute.

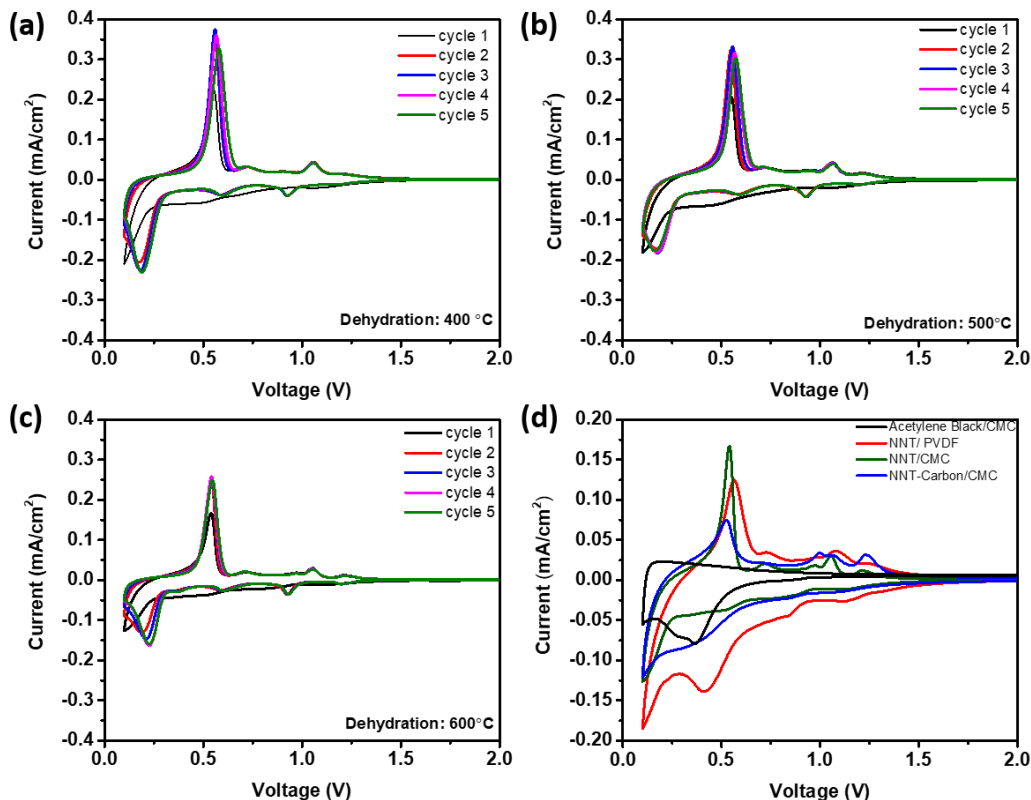


Fig. S4. (a-c) CV curves of half cells containing the dehydrated NNT samples heated to the indicated temperatures using CMC binder in the electrodes, at a scan rate of 0.5 mV/s. (d) First CV curves of half-cells containing NNT electrodes made with PVDF or CMC binders, and C-

coated NNT electrodes with CMC binder. Also shown is a CV curve of a blank electrode made with acetylene black.

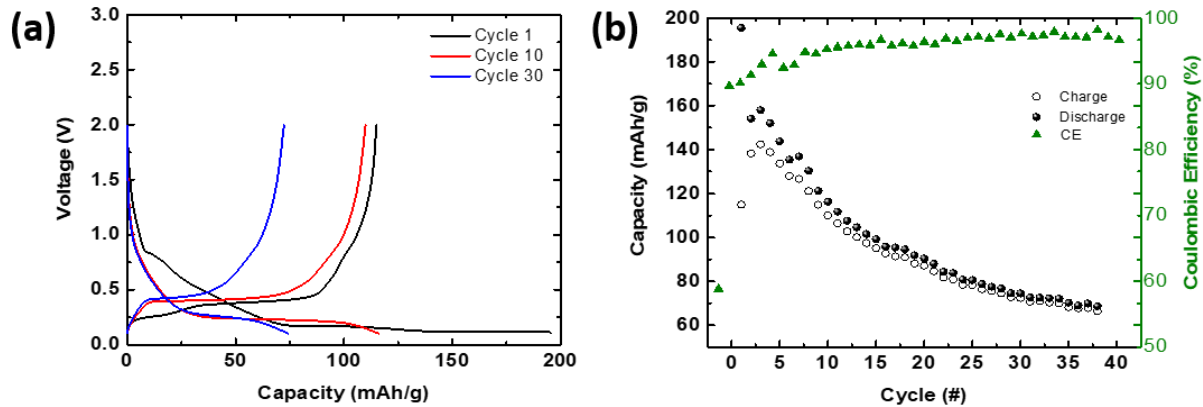


Fig. S5. The potential versus specific capacity profile for a half-cell containing carbon-coated NNT dehydrated at 800 °C cycled between 1.5 and 0.1 V at 0.15 mA cm⁻² (15 mA g⁻¹) (a), specific discharge and charge capacities and Coulombic efficiencies as a function of cycle number (b).

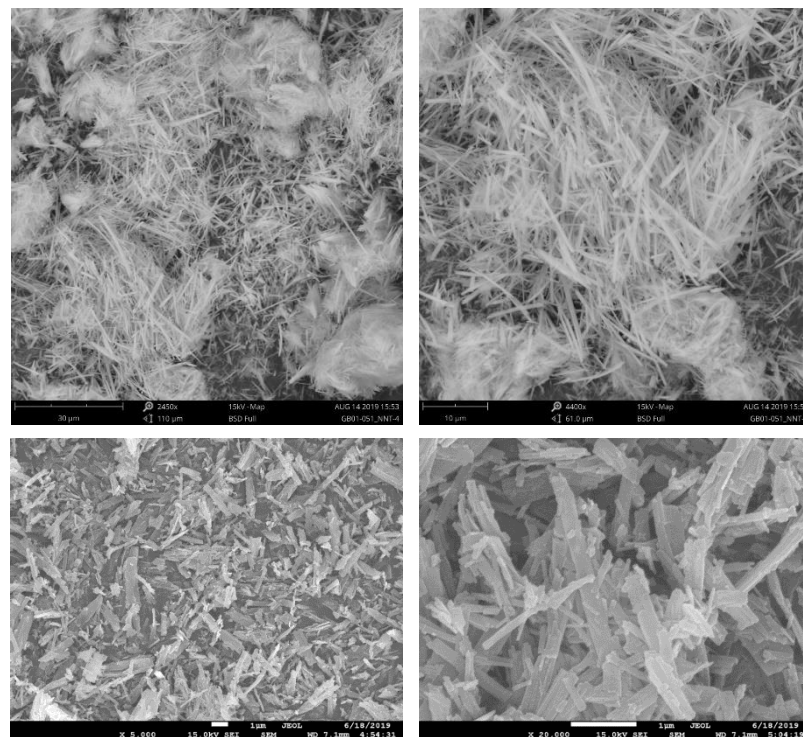


Fig. S6. SEM images of the as-prepared (top) and carbon coated (bottom) NNT samples.

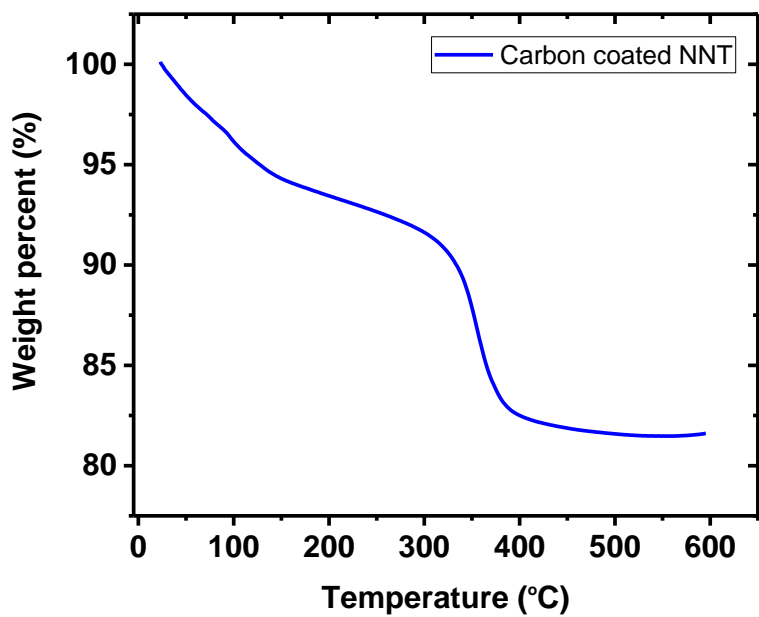


Fig. S7. Thermogravimetric analysis of carbon-coated NNT in air using a heating rate of 5 °C/minute.

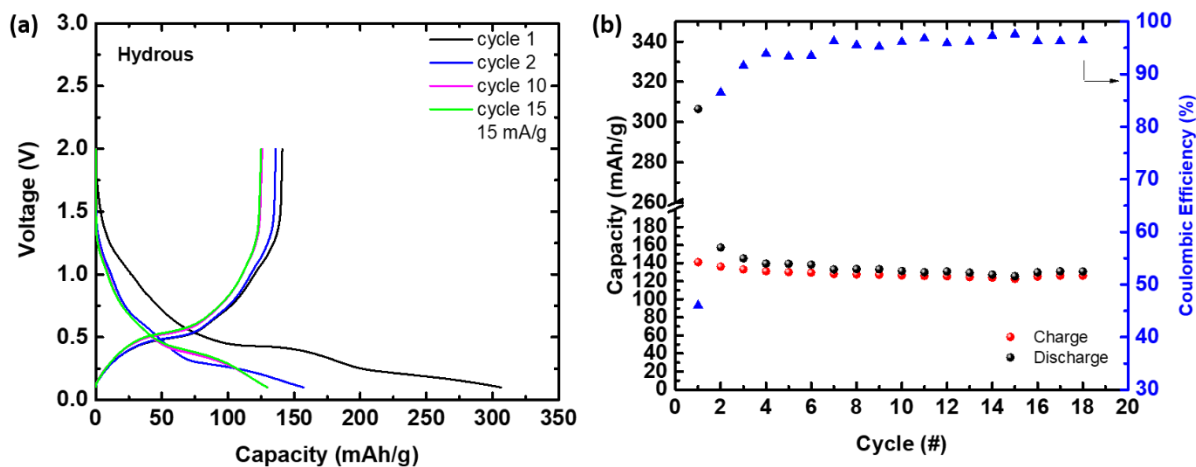


Fig. S8. The potential versus specific capacity profiles for the hydrous NNT samples in Na half-cells using CMC binder without C-coating **(a)** specific discharge and charge capacities and Coulombic efficiency as a function of cycle number **(b)**. The cell cycled between 2.0 and 0.1 V at 0.15 mA cm⁻² (15 mA g⁻¹).

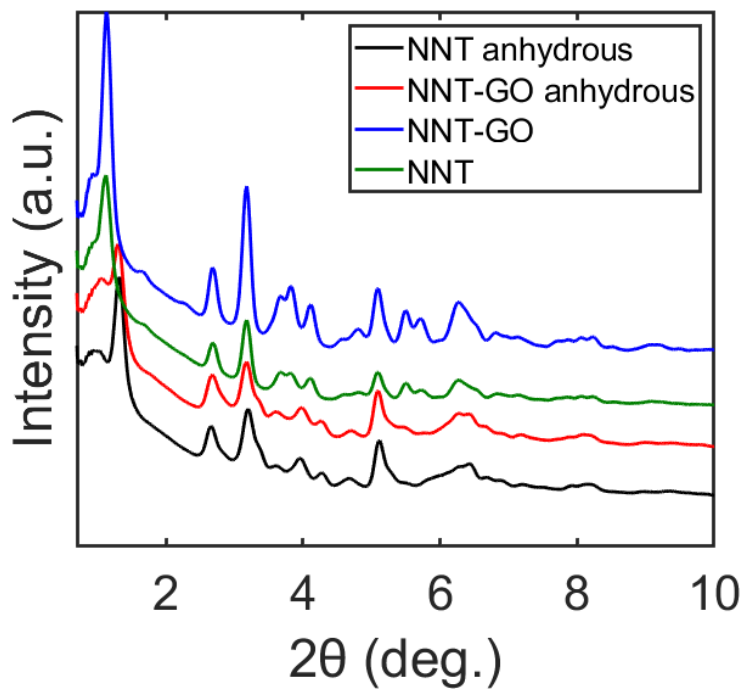


Fig. S9. Synchrotron XRD patterns of as prepared NNT and anhydrous NNT (annealed at 600 °C) with and without graphene (GO) wrapping.

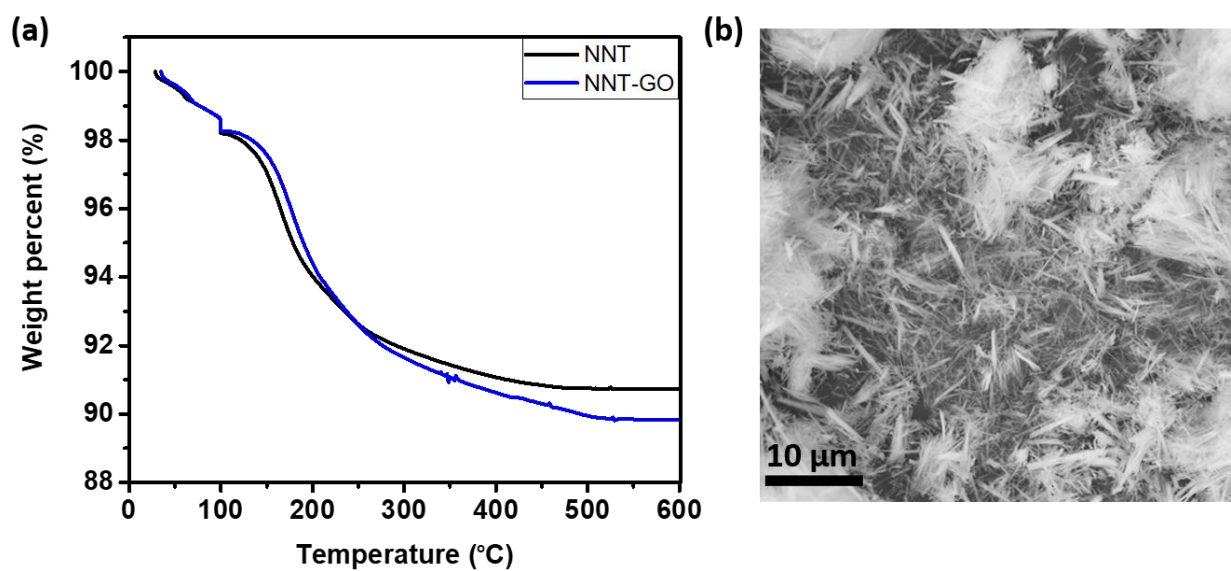


Fig. S10. (a) Thermogravimetric analysis of NNT-GO in air using a heating rate of 5 °C/min. (b) SEM micrograph of NNT-GO sample.

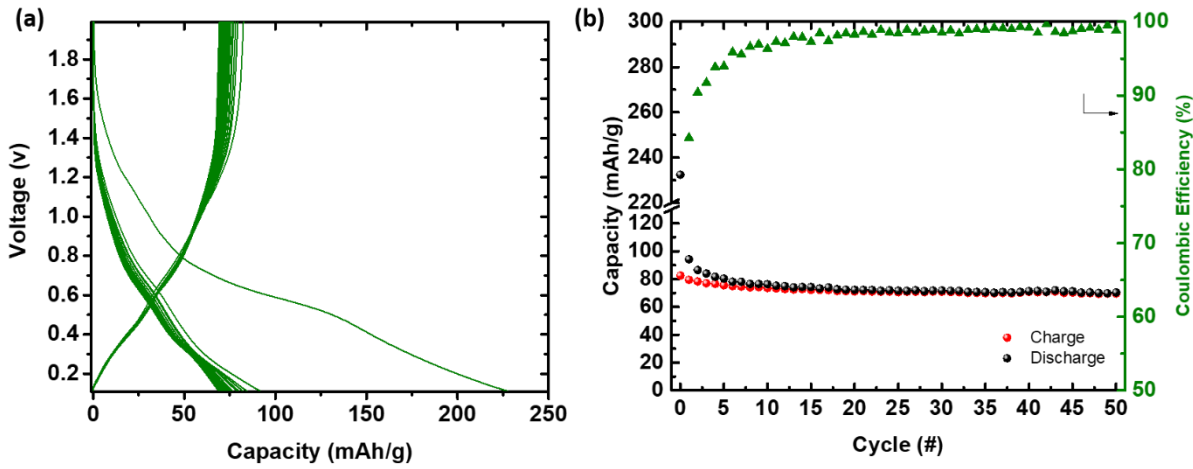


Fig. S11. The potential versus specific capacity profile for half-cells containing the graphene-wrapped NNT samples dehydrated at 500 °C in Na half-cells cycled between 2.0 and 0.1 V at 0.15 mA cm⁻² (15 mA g⁻¹) using PVDF binder **(a)**, specific discharge and charge capacities and Coulombic efficiency as a function of cycle number **(b)**.

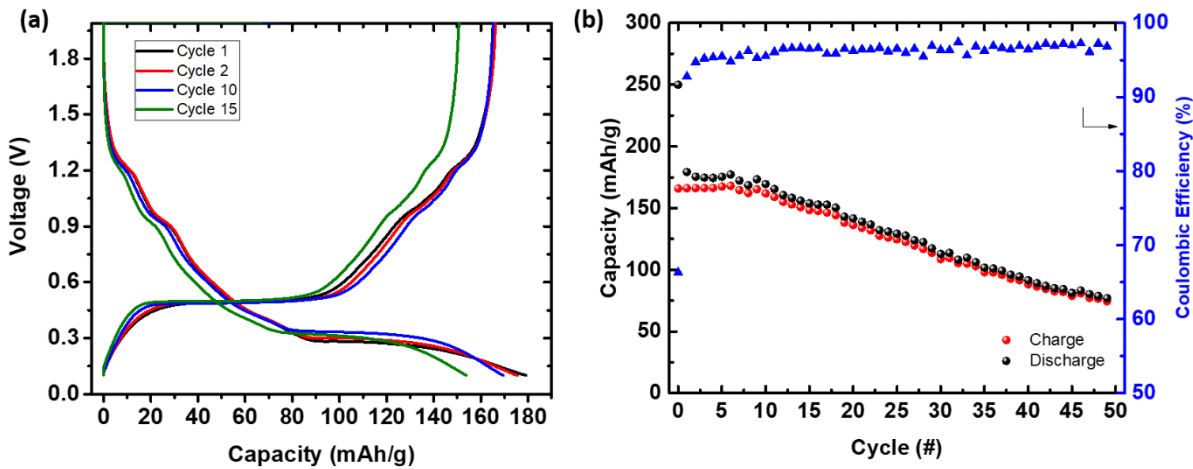


Fig. S12. The potential versus specific capacity profile for cells containing the graphene-wrapped NNT samples dehydrated at 500 °C in Na half-cells cycled between 2.0 and 0.1 V at 0.15 mA cm⁻² (15 mA g⁻¹) using CMC binder **(a)**, specific discharge and charge capacities and Coulombic efficiency as a function of cycle number **(b)**.

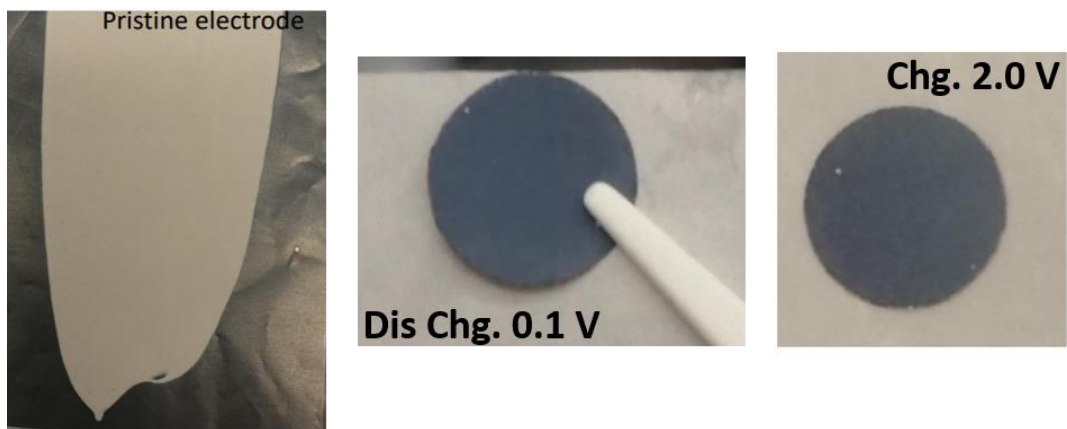


Fig. S13. Optical images of carbon-free pristine and cycled electrodes in different states of charge and discharge.